

Effect of Corner Modification on Forced Convection and Properties of Flowing Fluid Past Static Equilateral Triangular Prism at Various Reynolds Numbers

Tooba Ashfaq^{1*}, Shehryar Manzoor²

¹ Department of Mechanical Engineering, University of Engineering and Technology Taxila, Pakistan

² Department of Mechanical Engineering Technology, National Skills University, Islamabad, Pakistan

Abstract. This paper demonstrates the 2D numerical investigation to determine outcome of corner modification on the heat transfer and flow parameters of fluid flowing past static equilateral triangular prism. For this purpose, the corners are modified in such a way that 1/8 of the side length of prism is chamfered and rounded. Prism is placed in incompressible flow in such a way that one of its vertices is facing the upstream. Flow velocity varies as Reynolds number range from 50 to 150 with an increment of 20. Drag and lift coefficients are sensitive to corner profile of prism. At Re of 110, rounding caused a maximum of 6.5% and 12.6% reduction is observed after chamfering the corners of prism. Increasing Re caused Root mean square value of lift coefficient (C_{LRMS}) to increase. At Re of 150, chamfered corners increased the C_{LRMS} by 22.3% whereas rounding enhanced it by 21.6%. Time-averaged streamlines suggested the reduction in the wake width behind the prism with increasing Re and changed corner profile. Forced convective heat transfer from sharp, rounded and chamfered prisms is discussed in terms of time and space averaged Nusselt number which enhanced by 5% after corner modification of prism. Lastly, mean spread of heat transfer coefficient over prisms is presented and discussed.

Keywords: corner modification, equilateral triangular prism, rounding, chamfering, streamlines, drag coefficient, lift coefficient, Nusselt number, surface heat transfer coefficient

1 Introduction

Fluid-structure interaction is crucial in understanding, designing and optimizing many engineering systems such as wind turbines, ships, offshore structures and aircraft wings that are more efficient and durable. The study of this interaction is of supreme importance to

* Corresponding author: toobaashfaq.uet@gmail.com

tackle natural disasters by understanding the behavior of waves and the response of structures to extreme events like tsunamis, hurricanes and earthquakes. When fluid flows over a structure with sharp corners such as a square, rectangular or triangular prism, fluid separates from the surface leading to large pressure differences and turbulence which ultimately increases the drag on the surface. Sharp corners can also lead to the formation of vortices that can cause vibration in structure which leads to fatigue failure or damage over time. Fluid cavitation is another problem in which bubbles and voids are formed in the fluid due to low pressure caused by sharp corners. Therefore, to mitigate these problems caused by sharp corners of structures, several studies have explored the corner modification effect on the heat transfer and fluid flowing past a structure. Tamura and Miyagi[1] reported the outcome of corner rounding and chamfering for square cylinder in air cross flow and concluded a reduction in drag forces due to wake width reduction. Alonso and Meseguer[2] studied the effect of corner roundness by rounding two corners of triangular prism and placed it in such a way that rounded corners came upstream at higher Reynolds number. It was observed that corner roundness significantly reduced the galloping instability of prism. Also, a direct relationship between corner roundness and reduction in instability was observed. Ambreen and Kim[3] numerically observed the decrease in coefficient of drag and amplification of heat transfer properties at $55 \leq Re \leq 200$, when corners of square prism was modified to rounded, chamfered and recessed corners. Daemei and Eghbali[4] numerically proved 50% reduction in wake region by modifying the corners of a triangular building to rounded, chamfered and recessed corners subjected to air cross flow. Effect of corner roundness was deeply studied by Alam et al.[5] where a square cylinder was modified to a circular one. Results suggested an enhancement of 37% in heat transfer properties as a result of corner roundness. Li et al.[6] further reported reduction in wind load over buildings having square cross section as a result of corner modification i.e., (chamfered and recessed). Du et al.[7] numerically analysed six shape modifications of square cylinder and concluded that aerodynamic forces are reduced in case of round corners and convex sides whereas round cornered concave sides enhance the aerodynamic forces/wind loading.

To the best of author's knowledge, vertex modification effect on heat transfer and flow of incompressible fluid past a stationary equilateral triangular prism has not been explored till now. Therefore, this research work aims at determining the outcome of corner rounding and chamfering on the forced convection and incompressible transient flow of fluid past a static equilateral triangular prism, positioned in such a way that one of its vertices faces the upstream, at a range Reynolds number i.e., $50 \leq Re \leq 150$.

2 Problem Statement

2D numerical investigation is done to determine the corner alteration effect on the properties of flowing fluid and heat transfer from a static equilateral triangular prism. For this purpose, the corners are modified in such a way that 1/8 of the side length of prism is chamfered and rounded. Prism is placed in incompressible flow in such a way that one of its vertices is facing the upstream. Flow velocity varies as Reynolds numbers range from 50 to 150 with an increment of 20. Outcome of corner modification on fluid flow past the prism are demonstrated in the form of time and space averaged coefficient of drag (C_{Dmean}) and root mean square value of coefficient of lift (C_{LRMS}), Strouhal number (St) and time averaged spread of pressure coefficient (C_{pmean}) on the prism surface. Moreover, time-averaged velocity streamlines are presented and discussed. Forced convection heat transfer from sharp, rounded and chamfered prisms is discussed in terms of time and space averaged Nusselt number and time-averaged distribution of surface heat transfer coefficient.

3 Governing Equations

The equations responsible for flow and heat transfer from prism are as follows:

Continuity Equation:

$$\frac{\partial u}{\partial x} + \frac{\partial v}{\partial y} = 0 \tag{1}$$

Conservation of inline momentum:

$$\frac{\partial u}{\partial t} + \frac{\partial u^2}{\partial x} + \frac{\partial vu}{\partial y} = -\frac{\partial p}{\partial x} + \frac{1}{Re} \left(\frac{\partial^2 u}{\partial x^2} + \frac{\partial^2 u}{\partial y^2} \right) \tag{2}$$

Conservation of transverse momentum:

$$\frac{\partial v}{\partial t} + \frac{\partial vu}{\partial x} + \frac{\partial v^2}{\partial y} = -\frac{\partial p}{\partial y} + \frac{1}{Re} \left(\frac{\partial^2 v}{\partial x^2} + \frac{\partial^2 v}{\partial y^2} \right) \tag{3}$$

Energy Equation:

$$\frac{\partial T}{\partial t} + u \frac{\partial T}{\partial x} + v \frac{\partial T}{\partial y} = \alpha \left(\frac{\partial^2 T}{\partial x^2} + \frac{\partial^2 T}{\partial y^2} \right) \tag{4}$$

where, u and v refer to non-dimensional streamwise and transverse components of velocity normalized by free stream velocity i.e., U_∞ . T is non-dimensional temperature normalized by free stream temperature (T_∞) and α refers to thermal diffusivity.

3.1 Boundary Conditions

At inlet: $u = U_\infty, v = 0, T = T_\infty$ (5)

At outlet: $p = 0$ (6)

At surface of prism: $u = 0, v = 0, T = T_c = \text{constant}$ (7)

where, T_c refers to the wall temperature of prism.

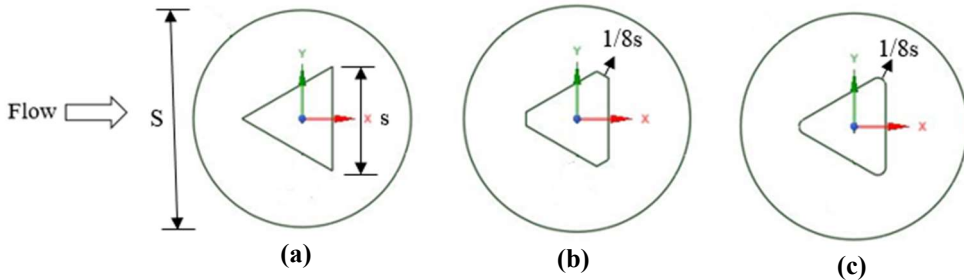


Fig 1. Illustrative diagram of stationary prism having (a) sharp, (b) chamfered and (c) rounded corners

4 Independence Study

For domain size independence, numerical simulations are performed on three different circular domains i.e., $S=80s, 160s$ and $240s$ where ‘ s ’ refers to the edge length of triangular prism. Radial x circumferential nodes and time step size (Δt) are fixed at 204×240 and 0.0001 respectively. Mesh is built in such a way that it is concentrated near the wall of prism. Maximum deviation between S1 and S2 is found to be 18% in CL_{RMS} whereas it is 2% between S2 and S3. Hence, the results are converged at S2.

Grid independence study is performed by choosing optimal mesh concentration where results are converged. For this purpose, three grids are tested i.e., Coarse ($G1$, circumferential x radial = 180×210), Medium ($G2 = 204 \times 240$) and Fine ($G3 = 235 \times 280$) for fixed Domain

size of $S_2=160s$ and Δt of 0.0001. Results suggest a maximum difference of 10.8% between G1 and G2 in the C_{LRMS} . C_{LRMS} deviation between G2 and G3 is 2.8%. Hence, for better accuracy of results, G2 is chosen for further simulations.

After domain size and grid independence study, time step size independence is performed by testing three different time step sizes i.e., Δt of 0.00005, 0.0001 and 0.0005 at fixed domain size of 160s and grid of 204x240. Maximum deviation between Δt_1 and Δt_2 is 20.4% in C_{LRMS} . Between Δt_2 and Δt_3 , maximum deviation in C_{LRMS} is 3.1%. Hence, results are proven to be converged at Δt_2 .

Hence, through a careful independence study, a computational domain of 160s having grid of 204 x 240 concentrated near the prism wall simulated at a time interval of 0.0001 is chosen for extended thermal and fluid flow analysis past stationary equilateral triangular prism with sharp, rounded and chamfered corners.

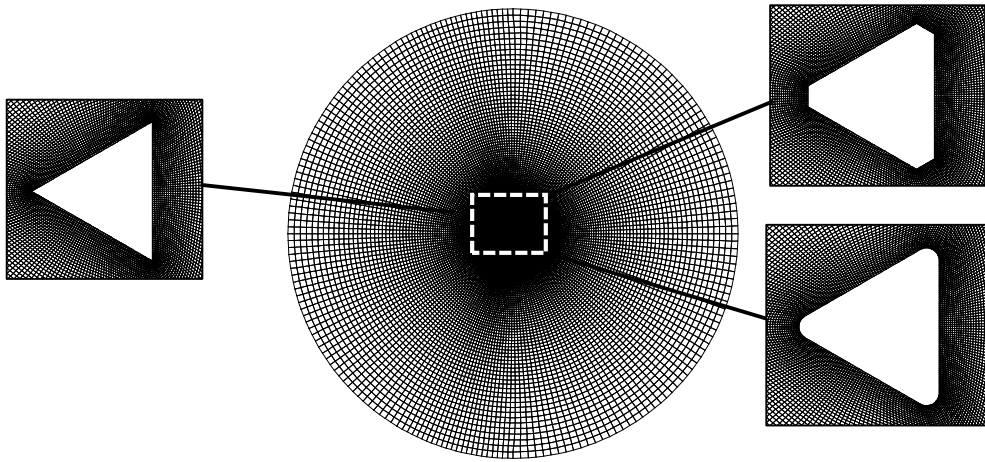


Fig 2. Complete grid with zoomed in view of prism with sharp, chamfered and rounded corners.

5 Validation of Numerical Model

This section validates the computational model devised after careful independence study. Here, the results for flowing fluid across a static sharp cornered equilateral triangular prism are compared with the results obtained by Tu et al. [8] for $50 \leq Re \leq 150$ in terms of C_{Dmean} , C_{LRMS} and St where prism is placed in such a way that one of its vertices face the upstream. Furthermore, heat transfer from sharp cornered triangular prism is validated with following expression presented by Chatterjee and Mondal [9], where Nusselt number is expressed in terms of Reynolds number for $50 \leq Re \leq 150$ and $Pr=6.9$.

$$Nu_{mean} = 0.539 \times Re^{0.5808} \times Pr^{1/3} \quad (8)$$

Figure 3(a) compares the C_{Dmean} for sharp cornered prism with that of the available literature and maximum deviation of 3.9% is observed at Re of 150. Maximum deviation of 2.5% is found in C_{LRMS} , when compared with the literature in Figure 3(b). Similarly, in Figure 3(c), present results are compared with that of existing literature comparison of present results for Strouhal number that yielded a maximum deviation of 5% at Re of 160. Comparison of Nu_{mean} is shown in Figure 3(d) where present results deviate from the results obtained by Chatterjee and Mondal [2] by 4% at Re of 50. There is a very insignificant difference in the results previously published and the present ones. So, it can be stated that the present numerical model is in line with the existing literature.

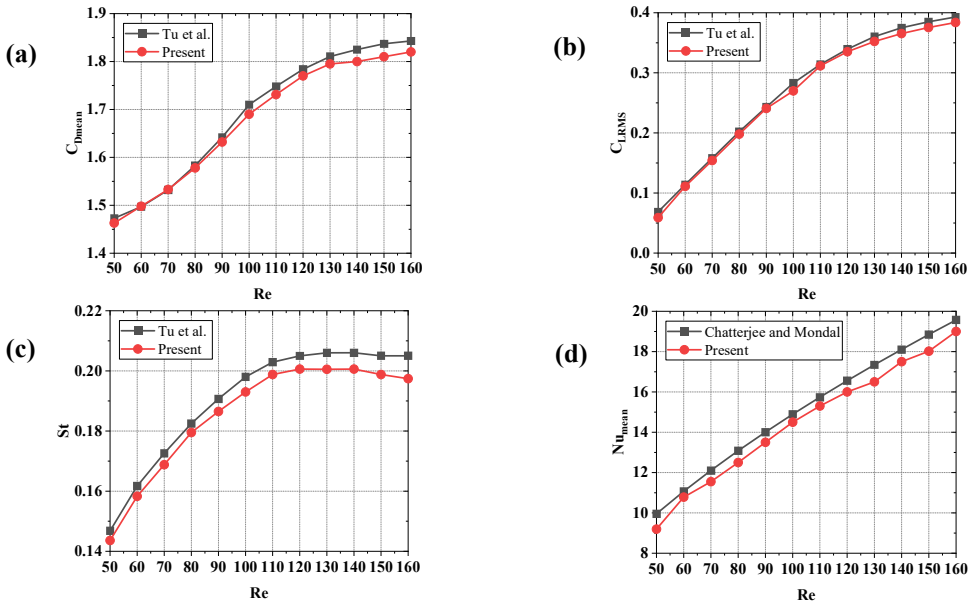


Fig 3. Comparison of present results with available literature of (a) C_{Dmean} , (b) C_{LRMS} , (c) St and (d) Nu_{mean}

6 Results and Discussion

In this portion, the outcome of corner modification on the properties of flowing fluid and heat transfer from static equilateral triangular prism is discussed where the velocity of incoming flow changes as Reynolds number varies in the range of 50 to 150 with an increment of 20. Here, fluid flow is analyzed on the basis of C_{Dmean} , C_{LRMS} , St , time-averaged velocity streamlines and time-averaged coefficient of pressure C_{Pmean} spread on the surface of prisms at described range of Reynolds numbers. Heat transfer properties are assessed on the basis of space and time-averaged Nusselt number and time-averaged heat transfer coefficient spread on the surface of all the three prisms.

6.1 C_{Dmean} , C_{LRMS} , St and Nu_{mean}

In Figure 4(a-c), change of C_{Dmean} , C_{LRMS} and St respectively with respect to Reynolds number (Re) for static equilateral triangular prisms having sharp, rounded and chamfered corners is shown. In Figure 4(a), it is observed that within the examined range of Reynolds number, C_{Dmean} increases with increase in Re . For sharp cornered prism, C_{Dmean} is consistently higher as compared to chamfered and round cornered prisms. After rounding the corners, maximum reduction of 6.5% is observed at Re of 110. However, chamfering reduced the mean value of drag coefficient to about 12.6% at Re of 110. Variation of C_{LRMS} with respect to Reynolds number for sharp, rounded and chamfered prisms is shown in Figure 4(b) where C_{LRMS} is observed to increase with increasing Re . It may be noted that at $50 \leq Re \leq 110$, there is no significant difference in C_{LRMS} for sharp, rounded and chamfered prisms. But as Re increases further, i.e., within $110 < Re \leq 150$, the value of C_{LRMS} for chamfered and rounded prism surpasses the value of C_{LRMS} for sharp cornered prism. For sharp cornered prism, maximum C_{LRMS} is observed at Re of 150 where its value corresponds to 0.37 which is enhanced by 22.3% and 21.6% after chamfering and rounding the corners respectively.

Figure 4(c) presents the change that occurs in Strouhal number with respect to Re for sharp, rounded and chamfered prisms. St is found to increase with increasing Re. After corner modifications, a decrease in the non-dimensional vortex shedding frequency is observed within $50 \leq Re \leq 110$. Maximum reduction in St is found to be 4.36% and 5.57% at Re of 50 after rounding and chamfering the corners respectively. As Re increases further, i.e. within $110 < Re \leq 150$, Strouhal number is found to be increased by 1.77% at Re of 150 when corners are rounded. Chamfered corners provided 6.58% increase in vortex shedding frequency at Re of 150. Figure 4(d) shows the change that occurs in time and space averaged value of Nusselt number (Nu_{mean}) in terms of Reynolds number for sharp, rounded and chamfered cornered prisms. With increasing Reynolds number, the value of Nu_{mean} also increases. For sharp cornered prism, maximum value of Nu_{mean} lies at Re of 150 where its value corresponds to 18.019. After rounding and chamfering the corners of prism, Nu_{mean} is observed to increase by 5%. There is no significant difference between the values of Nu_{mean} for chamfered and rounded prisms at examined range of Reynolds number.

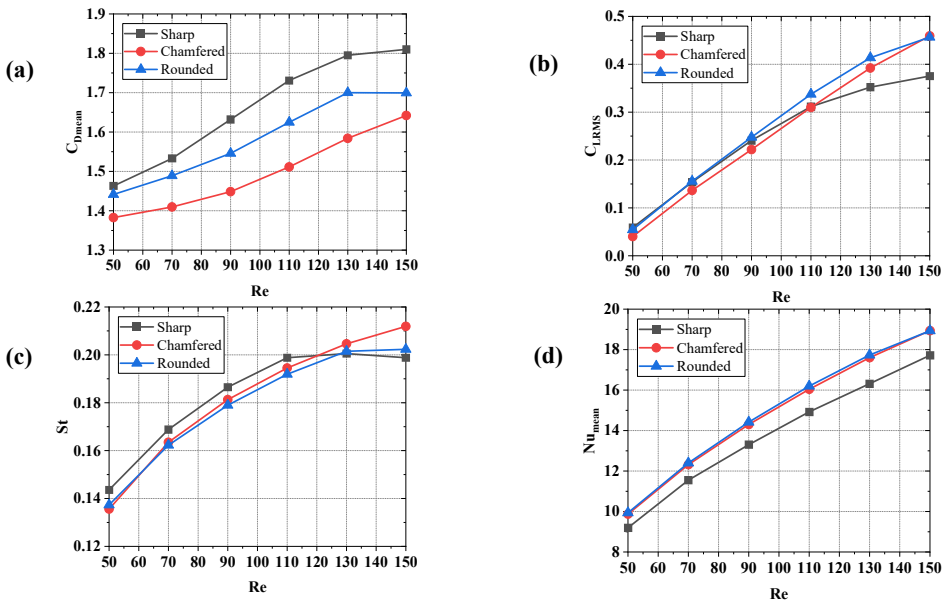


Fig 4. Variation of (a) C_{Dmean} , (b) C_{LRMS} and (c) St and (d) Nu_{mean} with respect to Reynolds number for stationary equilateral triangular prisms having sharp, rounded and chamfered corners

6.2 C_{Pmean} distribution on the surface of prisms

Figure 5(a-c) shows the time-averaged distribution of pressure coefficient at various Reynolds numbers on the surface of equilateral triangular prism having sharp, rounded and chamfered corners respectively. It is evident that C_{Pmean} is sensitive to both Reynolds number and corner profiles. In Figure 5(a), Vertex B faces the incoming flow of fluid. Here, the value of C_{Pmean} is maximum as it is the forward stagnation point. Along the edges B-A and B-C, C_{Pmean} reduces and achieves a negative value indicating the formation of wake region. At the rear edge i.e. A-C, with increasing Reynolds number, the value of C_{Pmean} becomes more negative. For round and chamfered cornered prism, as shown in Figure 5(b) and (c), the forward stagnation point is not as distinct as in the case of sharp cornered prism because of corner profile i.e., roundness and chamfering of corners respectively. However, it is still evident that it lies between C and D points as C_{Pmean} is maximum between C and D. It is to note that for all prisms, the maximum value of C_{Pmean} at forward stagnation point of prisms

decreases as Reynolds number increases from 50 to 150. The value of C_{Pmean} at rear edge of prism also gets more negative with increasing Reynolds number. After corner modification, it is observed that maximum C_{Pmean} at forward stagnation point is lower for rounded and chamfered prism than that in case of sharp cornered prism.

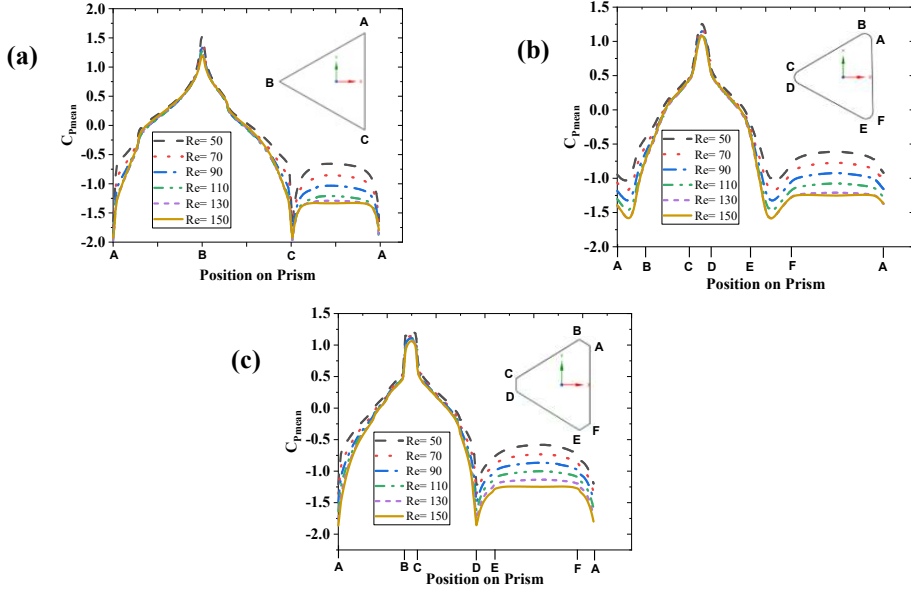


Fig 5. C_{Pmean} spread on the surface of static equilateral triangular prisms having (a) sharp, (b) rounded and (c) chamfered corners at various Reynolds numbers

6.3 Time-Averaged Streamlines:

In Figure 6, the time-averaged velocity streamlines for sharp, rounded and chamfered cornered prism at $50 \leq Re \leq 150$. The flow around the edges of prism produces vortices which can cause forces on prism. Because of these vortices, flow separates from the surface of prism, leading to large pressure differences. In case of a prism having equilateral triangular cross section, fluid flow can typically be divided into two regions: the flow over the prism and the flow under the prism. The flow over the prism can produce large wake region behind the prism, while flow under the prism causes vortices to form at corners of prism. In Figure 6, for sharp, rounded and chamfered prisms, it is evident that maximum length of wake region is obtained at Re of 50. As Reynolds number increases from 50 to 150, length of wake region significantly reduces to a minimum length at Re of 150. Wake region is also sensitive to corner profile of prism as it is seen in Figure 6 (from left to right), where rounding and chamfering the corners of prism, reduced the region where flow separates from the surface of prism. It is because of the fact that rounded and chamfered prisms do not have sharp corners where flow separates from the surface. Instead of that, due to modified corner profiles, flow follows the rounded and chamfered profile and flow separation is delayed.

Hence, time-averaged streamlines are sensitive to both, Reynolds number and corner profiles.

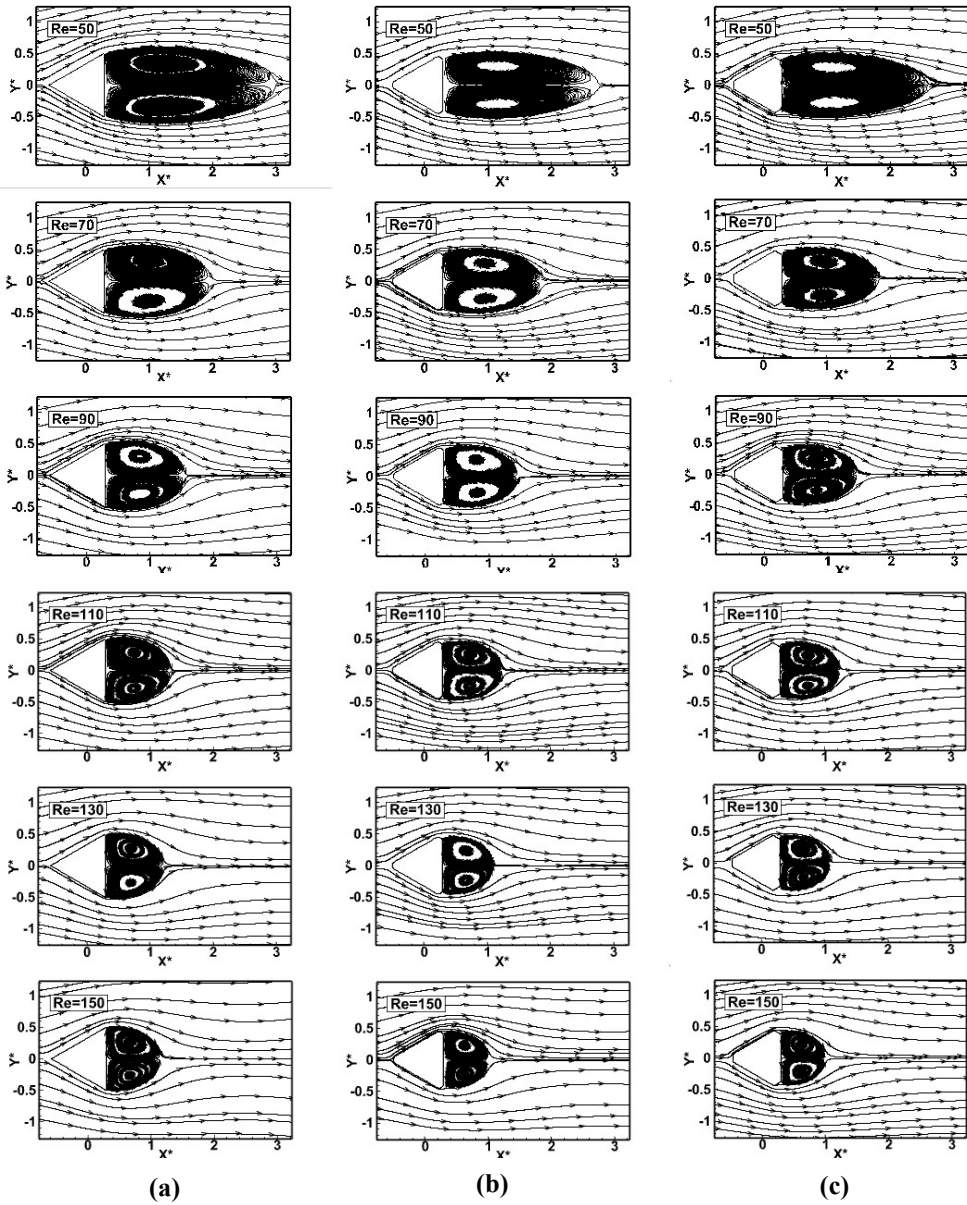


Fig 6. Time Averaged Streamlines for static equilateral triangular prism having (a) sharp, (b) rounded and (c) chamfered corners at various Reynolds numbers

6.4 Mean heat transfer coefficient (h_{mean}) spread over prisms

Figure 7(a-c) shows the distribution of h_{mean} on prism with sharp, rounded and chamfered corners respectively. It is evident from the Figure 7(a) that h_{mean} is highest at the vertex B that is upstream the fluid as fluid is totally in contact with prism there. As flow moves away from the upstream point, towards the edges B-A and B-C, h_{mean} starts declining and then reduce to its local minima at the downstream edge of prism i.e., A-C, where fluid separates from the prism and recirculation occurs. In Figure 7(b), for rounded cornered prism, transitioning from

one point to the other is smooth because of corner curvature. In figure 7(c), for chamfered cornered prism, it is seen that maximum h_{mean} is found at upstream corners i.e., C and D because vertices provide more skin friction than edge C-D. Hence, instead of one peak value of h_{mean} for sharp and rounded prisms, two peaks are observed in case of chamfered prism. Moreover, as Reynolds number increases, h_{mean} experiences a significant enhancement in case of all the three prisms.

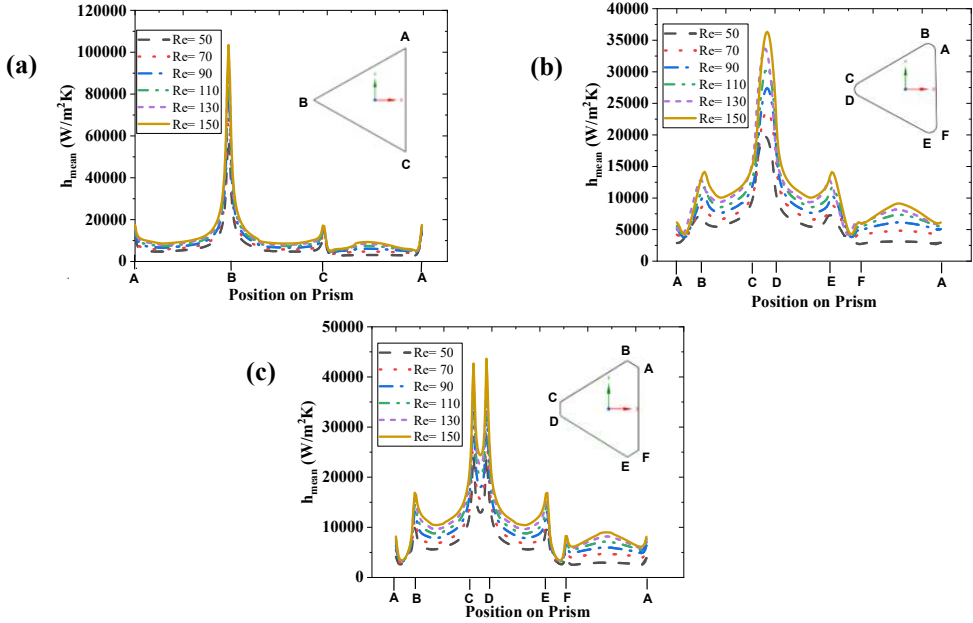


Fig 7. Time-averaged spread of heat transfer coefficient over stationary equilateral triangular prism having (a) sharp, (b) rounded and (c) chamfered corners at $50 \leq Re \leq 150$

7 Conclusions:

Following conclusions are drawn after careful numerical analysis of a stationary equilateral triangular prism with sharp, rounded and chamfered corners placed in an incompressible fluid flow at $50 \leq Re \leq 150$ in such a way that one of its vertices faces the upstream.

1. C_{Dmean} and C_{LRMS} are sensitive to corner modification of prism. Maximum reduction in C_{Dmean} is found to be 6.5% and 12.6% at Re of 110 after rounding and chamfering the corners respectively. C_{LRMS} is observed to enhance by 21.6% and 22.3% when corners of the prism are rounded and chamfered respectively.
2. Re is inversely related to C_{Pmean} on the surface of prism. The profile of C_{Pmean} distribution on the surface of rounded and chamfered prism is seen to be lower than that on the surface of sharp cornered prism.
3. Time averaged streamlines are sensitive to both Reynolds number and corner profile of equilateral triangular prism. With increasing Reynolds number, wake width is found to reduce. Rounding and chamfering delayed the fluid separation and consequently reduced the wake width behind prism.
4. Nu_{mean} is directly related to Reynolds number and it increases by 5% as a result of corner modification of prism at Re of 150.
5. h_{mean} distribution on the surface of prisms suggested a higher value of h_{mean} at vertices as compared to edges. h_{mean} enhanced with increase in Re.

References

- [1] T. Tamura and T. Miyagi, "The effect of turbulence on aerodynamic forces on a square cylinder with various corner shapes," *Journal of Wind Engineering and Industrial Aerodynamics*, vol. 83, no. 1-3, pp. 135-145, 1999.
- [2] G. Alonso and J. Meseguer, "A parametric study of the galloping stability of two-dimensional triangular cross-section bodies," *Journal of Wind Engineering and Industrial Aerodynamics*, vol. 94, no. 4, pp. 241-253, 2006.
- [3] T. Ambreen and M.-H. Kim, "Flow and heat transfer characteristics over a square cylinder with corner modifications," *International Journal of Heat and Mass Transfer*, vol. 117, pp. 50-57, 2018.
- [4] A. B. Daemei and S. R. Eghbali, "Study on aerodynamic shape optimization of tall buildings using architectural modifications in order to reduce wake region," *Wind and Structures*, vol. 29, no. 2, pp. 139-147, 2019.
- [5] M. M. Alam, T. Abdelhamid, and A. Sohankar, "Effect of cylinder corner radius and attack angle on heat transfer and flow topology," *International Journal of Mechanical Sciences*, vol. 175, p. 105566, 2020.
- [6] Y. Li, X. Tian, K. F. Tee, Q.-S. Li, and Y.-G. Li, "Aerodynamic treatments for reduction of wind loads on high-rise buildings," *Journal of Wind Engineering and Industrial Aerodynamics*, vol. 172, pp. 107-115, 2018.
- [7] X. Du, D. Shi, H. Dong, and Y. Liu, "Flow around square-like cylinders with corner and side modifications," *Journal of Wind Engineering and Industrial Aerodynamics*, vol. 215, p. 104686, 2021.
- [8] J. Tu, D. Zhou, Y. Bao, Z. Han, and R. Li, "Flow characteristics and flow-induced forces of a stationary and rotating triangular cylinder with different incidence angles at low Reynolds numbers," *Journal of Fluids and Structures*, vol. 45, pp. 107-123, 2014.
- [9] D. Chatterjee and B. Mondal, "Forced convection heat transfer from an equilateral triangular cylinder at low Reynolds numbers," *Heat and Mass Transfer*, vol. 48, no. 9, pp. 1575-1587, 2012.